BULLETIN OF THE POLISH ACADEMY OF SCIENCES
TECHNICAL SCIENCES
Vol. 53, No. 2, 2005

Growth of MOCVD HgCdTe heterostructures for uncooled infrared photodetectors

A. PIOTROWSKI[1], P. MADEJCZYK[2], W. GAWRON[2], K. KŁOS[1], J. PAWLUCZYK[1], M. GRUDZIEŃ[1], J. PIOTROWSKI[1], and A. ROGALSKI[2]*

[1]VIGO System S.A., 3 Świetlików Str., 01-389 Warsaw, Poland
[2]Institute of Applied Physics, Military University of Technology, 2 Kaliskiego Str., 00-908 Warsaw, Poland

Abstract. In the paper recent progress at VIGO/MUT (Military University of Technology) MOCVD Laboratory in the growth of $Hg_{1-x}Cd_xTe$ (HgCdTe) multilayer heterostructures on GaAs/CdTe substrates is presented. The optimum conditions for the growth of single layers and complex multilayer heterostructures have been established. One of the crucial stages of HgCdTe epitaxy is CdTe nucleation on GaAs substrate. Successful composite substrates have been obtained with suitable substrate preparation, liner and susceptor treatment, proper control of background fluxes and appropriate nucleation conditions. The other critical stage is the interdiffused multilayer process (IMP). The growth of device-quality HgCdTe heterostructures requires complete homogenization of CdTe-HgTe pairs preserving at the same time suitable sharpness of composition and doping profiles. This requires for IMP pairs to be very thin and grown in a short time.

Arsenic and iodine have been used for acceptor and donor doping. Suitable growth conditions and post growth anneal is essential for stable and reproducible doping. *In situ* anneal seems to be sufficient for iodine doping at any required level. In contrast, efficient As doping with near 100% activation requires *ex situ* anneal at near saturated mercury vapours. As a result we are able to grow multilayer fully doped (100) and (111) heterostructures for various infrared devices including photoconductors, photoelectromagnetic and photovoltaic detectors. The present generation of uncooled long wavelength infrared devices is based on multijunction photovoltaic devices. The technology steps in fabrication of devices are described. It is shown that near-BLIP performance is possible to achieve at ≈ 230 K with optical immersion. These devices are especially promising as 7.8–9.5-μm detectors, indicating the potential for achieving detectivities above 10^9 cmHz$^{1/2}$/W.

Key words: MOCVD growth, HgCdTe ternary alloy, room temperature infrared photodetectors.

1. Introduction

The common believe is that infrared photodetector needs to be cooled to achieve a high sensitivity. Detection of long wavelength infrared (LWIR) radiation, characterized by low photon energy, requires transitions of free charge carriers which have energy not much lower than the photon one. Therefore, at near room temperatures the thermal energy kT becomes comparable to the transition energy. The direct consequence of this is a very high rate of thermal generation of charge carriers. The statistical nature of this process generates signal noise. As a result LWIR detectors become very noisy when they operated at near room temperature. Cooling is a direct, straightforward, and very efficient way to suppress the thermal generation of charge carriers, being at the same time a very impractical method. The need for cooling is a major limitation of photodetectors, and inhibits the more widespread application of IR technology. Affordable high performance infrared imaging cameras, require cost-effective IR detectors that operate without cooling or, at least, at temperatures achievable by low power and low cost coolers. Since cooling requirements add considerably to the cost weight, power consumption and inconvenience of an IR system, it is highly desirable to eliminate or reduce the cooling requirements.

VIGO System S.A. has developed a number of types of unique photodetectors for short, medium and long wavelength IR radiation operating without cryogenic cooling [1–3]. Isothermal vapour phase epitaxy (ISOVPE) has been the base technology for HgCdTe growth for many years [1,4]. It is very mature and stable technique with a lot of limitations. Further improvement in detector performance requires application of more sophisticated devices which can be fabricated with advanced epitaxial techniques like metalorganic chemical vapour deposition (MOCVD) or molecular beam epitaxy (MBE).

This paper presents recent progress at VIGO/MUT MOCVD Laboratory in the growth of $Hg_{1-x}Cd_xTe$ (HgCdTe) multilayer heterostructures on GaAs/CdTe substrates for uncooled infrared photodetectors. The special attention is focused on the improvement in multijunction LWIR photovolatic detectors.

*e-mail: rogan@wat.edu.pl

2. Impact of epitaxial growth on development of HgCdTe detectors

The time line for the evolution of HgCdTe growth technologies is illustrated in Fig. 1. Historically, crystal growth of HgCdTe has been a major problem mainly because a relatively high Hg pressure is present during growth, which makes it difficult to control the stoichiometry and composition of the grown material.

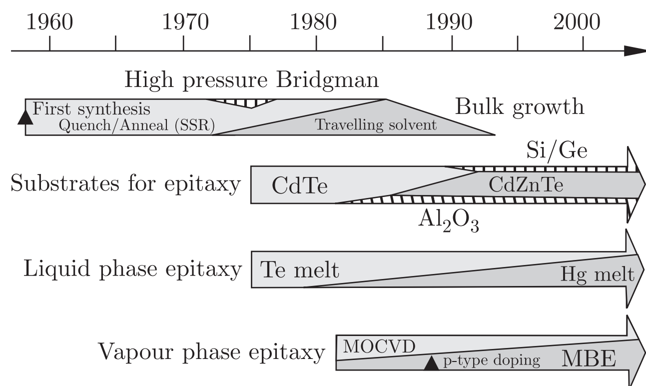

Fig. 1. Evolution of HgCdTe crystal growth technology from 1958 to present (after Ref. 5)

Early experiments and a significant fraction of early production were done using a quench-anneal or solid-state recrystalization process. Bridgman growth was attempted for several years near the mid-70s last century. At the same time, solvent growth methods from Te-rich melts were initiated to reduce the grown temperature. One successful implementation was the traveling heater method up to 5-cm diameter [6].

The bulk HgCdTe crystals were initially used for any types of infrared photodetectors. At present they are still used for some infrared applications such as n-type single element photoconductors, SPRITE detectors and linear arrays. Bulk growth produced thin rods, generally up to 15 mm in diameter, about 20 cm in length, and with non-uniform distribution of composition. Large two-dimensional arrays could not be realized with bulk crystals. Another drawback to bulk material was the need to thin the bulk wafers, generally cut about 500-μm thick, down to final device thickness of about 10 μm. Also further fabrication steps (polishing the wafers, mounting them to suitable substrates, and polishing to the final device thickness) were intensive labour.

The epitaxial techniques offer, in comparison with bulk growth techniques, the possibilities to grow large area epilayers and sophisticated device structures with good lateral homogeneity, abrupt and complex composition and doping profiles, which can be configured to improve the performance of photodetectors. The growth is performed at low temperatures, which makes it possible to reduce the native defects density. The properties of HgCdTe grown by the variety of techniques are summarized in Table 1.

Among various epitaxial techniques, the liquid phase epitaxy (LPE) is the most matured method. At present the growth of HgCdTe by vapour phase epitaxy (VPE) is typically done by nonequilibrium methods: MOCVD, MBE, and their derivatives. The great potential benefit of MBE and MOCVD over the equilibrium methods is the ability to modify the growth conditions dynamically during growth to tailor band gaps, add and remove dopants, prepare surfaces and interfaces, add passivations, perform anneals, and even grow on selected areas of a substrate. The growth control is exercised with great precision to obtain basic materials properties comparable to those routinely obtained from equilibrium growth.

LPE growth of thin layer on CdTe substrates began in the early-to-mid 70's. Initially, Te solutions with dissolved Cd (Cd has a high solubility in Te) and saturated with Hg vapour were used to efficiently grow HgCdTe in temperature range 420–600°C. This allowed small-volume melts to be used with slider techniques which did not appreciably deplete during the growth run. Experiments with Hg-solvent LPE began in the late 70's. Because of the limited solubility of Cd in Hg, the volume of the Hg melts had to be much larger then Te melts (typically of about 20 kg) in order to minimize melt depletion during layer growth in temperature range 380–500°C. This precluded the slider growth approach and Hg-melt epitaxy has been developed using large dipping vessels.

Table 1
Comparison of various methods used to grow HgCdTe

	Bulk			Liquid phase epitaxy		Vapour phase epitaxy		
	SSR	Traveling heater method						
		HCT melt	Te melt	Hg melt	Te melt	ISOVPE	MOCVD	MBE
Temperature (°C)	950	950	500	350–550	400–550	500	275–400	160–200
Pressure (Torr)	150 000	150 000	760–8000	760–11400	760–8000	760	300–760	10^{-3}–10^{-4}
Growth rate (μm/hr)	250	250	80	30–60	5–60	1–10	2–10	1–5
Dimensions w (cm)	0.8–1.2 dia	0.8–1.2 dia	2.5 dia	5	5	1 dia	7.5 dia	7.5 dia
l (cm)	–	–	–	6	5	–	4	4
t (cm)	15	15	15	0.0002–0.0030	0.0005–0.012	0.001	0.0005–0.001	0.0005–0.001
Density of dis. (cm^{-2})	$<10^5$	–	$<10^5$	$<10^5$	$<10^5$–10^7		5×10^5–10^7	$<5\times10^4$–10^6
Purity (cm^{-3})	5×10^{14}	5×10^{14}	5×10^{14}	5×10^{14}	5×10^{14}	$\approx 1\times10^{15}$	$<1\times10^{15}$	$<1\times10^{15}$
n-type dop. (cm^{-3})	N/A	N/A	N/A	1×10^{14}–1×10^{18}	1×10^{15}–1×10^{16}	1×10^{15}	5×10^{14}–5×10^{18}	5×10^{14}–1×10^{19}
p-type dop. (cm^{-3})	N/A	N/A	N/A	1×10^{15}–1×10^{18}	1×10^{15}–5×10^{16}	1×10^{16}–1×10^{17}	3×10^{15}–5×10^{17}	1×10^{16}–5×10^{18}
X-ray r. c. (arc sec)	–	–	20–60	<20	<20	–	50–90	20–30
Uniformity (Δx)	<0.002	<0.004	<0.005	<0.002	<0.002	<0.001	±0.01–0.0005	±0.01–0.0006

In the early 90's, bulk growth was replaced by LPE and now it is very mature for production of the first- and second-generation detectors. LPE technique has been successfully used in fabrication of double layer heterojunction p-on-n photodiodes, where p^+ cap layer is formed using arsenic as the dopant. However, LPE technology is limited for a variety of advanced HgCdTe structures required for third generation detectors. LPE typically melts off a thin layer of the underlying material and each time an additional layer is grown as a result of relatively high growth temperature. Additionally, the gradient in x-value in the base layer of p^+-on-n junction can generate a barrier transport in certain cases due to interdiffusion. These limitations provided an opportunity for vapour phase epitaxy: MBE and MOCVD.

The era of MBE and MOCVD began in the early 80's by adopting both methods well established in the III-V semiconductor materials. Through the next decade a variety of metalorganic compounds were developed along with a number of reaction-chamber designs [7]. In the case of MBE, a specially designed Hg-source ovens were successfully designed to overcome the low sticking coefficient of Hg at the growth temperature [8] The growth temperature is less than 200°C for MBE but around 350–400°C for MOCVD, making it more difficult to control the p-type doping in the MOCVD due to formation of Hg vacancies at higher growth temperatures. The vacancies can be removed by a low (<200°C) temperature anneal, however.

However, in the case of MBE application, post growth annealing at high temperatures is necessary for activation of acceptor dopant. At present, MBE is the dominant vapour phase method for HgCdTe. It offers low temperature growth under ultrahigh vacuum environment, *in situ* n-type and p-type doping, and control of composition, doping and interfacial profiles. Although the quality of MBE material is not yet on a par with LPE, it has made tremendous progress in the past decade.

3. MOCVD system

One of the important advantages of MOCVD system is the possibility to use low-cost composite substrates (GaAs, Si, sapphire) as the viable alternative to costly CdZnTe substrates. This system does not require high vacuum for growth, is easier serviceable technique with larger throughput. Last, but not least, donor and acceptor doping at medium and high level, essential for near room temperature devices, is simpler with MOCVD. That is why we selected MOCVD as the technique of choice for uncooled MOCVD devices. Aixtron Aix-200 II–VI MOCVD system was purchased in 2004. Fast switching valves, high quality materials and proper reactor design allow us to run fully computer-controlled processes. Low to atmospheric pressure growth is possible. Drawback of this technique, in comparison with previously used ISOVPE one, is high cost of equipment and high toxicity of precursors which is prevented by an advanced safety system.

The MOCVD system was installed in March 2003. The laboratory infrastructure was constructed from the ground in cooperation between VIGO System S.A. and Military University of Technology. It took half a year to develop CdTe buffer layer technology. In November 2003, fully doped heterostructures for devices became available. Since then we develop optimum growth parameters for devices covering the whole 2–16-μm range. Until August 2004 we grew over 380 heterostructures. Most of them were experiments on fundamental growth parameters, only small percent of all runs was useful for production purposes.

Aixtron Aix-200 II–VI MOCVD system is a horizontal reactor customized for $Hg_{1-x}Cd_xTe$ growth on 2" wafers (see Fig. 2). Pd-cell purified hydrogen is used as a carrier gas. Between processes the system is filled with nitrogen fined by getter purifier. Liquid nitrogen is used as the nitrogen source.

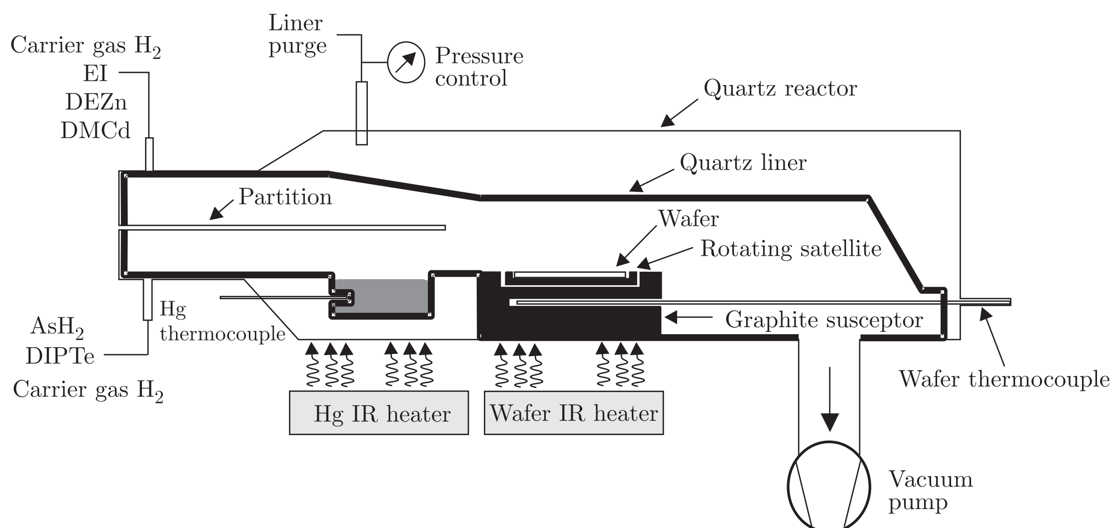

Fig. 2. Schematic drawing of Aix-200 II–VI reactor

Dimethylcadmium (DMCd), diisopropyltelluride (DIPTe) and diethylzinc (DEZn) used as precursors are held in temperature-stabilized baths. Elementary mercury is held in a quartz container in the lower input channel of the container. AsH_3 has been used as arsenic precursor. The drawback of arsine is its toxicity. Special safety preventive measures must have been applied to the laboratory. Ethyl iodide (EI) is used for donor doping. Because of its high vapour pressures, the metalorganic source for iodine must be held in low temperatures ($< 5°C$). DMCd/EI and DIPTe/AsH_3 input channels are separated to prevent premature gas mixing and dust formation. In the lower channel a mercury container is placed. Evapourating mercury is carried by hydrogen to the growth zone. Drawback of this solution is the dissolution of Te and As sources in the elementary mercury container. This may result in As memory effects. The surface of the mercury is covered with black skin, probably HgTe after deposition causing growth instabilities. Hydrogen from the upper channel dilutes mercury saturated hydrogen from the lower channel. Therefore, decrease in the mercury partial pressure over the wafer must be taken into account and it can be altered by changing the lower to upper channel flow ratio. In practice, the flow is selected separately for each phase; for example 100/500 sccm or 1200/1200 sccm flow ratios have been used. In this notation the first number is mass gas flow in the upper channel and the former is mass gas flow in the lower channel.

Two temperature zones are in the reactor: the mercury source zone (up to 300°C) and the growth zone with graphite susceptor (up to 900°C). Reactor temperatures 360–410°C have been used and mercury has been held in 200–220°C. Higher temperatures are used for reactor cleaning. Substrate is laying on a rotating disk using Aixtron's gas foil rotation technique. Vacuum system provides the possibilities to keep reactor at the pressures from 50 mbar to atmospheric pressure. Reactor pressure of 500 mbar was used for all successful growth runs.

MOCVD system contains explosive materials such as hydrogen and toxic materials as AsH_3, mercury and metalorganics precursors. Therefore, the laboratory is equipped with advanced safety feature devices such as hydrogen, arsine and mercury detectors, effective ventilation system and different safety interlocks embedded in the Aixtron's system. Large quantities of mercury are being transported during growth. They are condensed at low temperature Hg trap. Glovebox nitrogen atmosphere contains a lot of mercury and all its gas outlets are equipped with activated coal filters. All toxic gases are neutralized in the wet scrubber system.

4. CdTe buffer growth

CdTe buffer growth on GaAs is probably the most critical stage in HgCdTe growth due to lattice mismatch. For GaAs and CdTe, the mismatch is approximately 14.3%. So huge mismatch is neutralized by 2–10-μm thick CdTe buffer. The buffer plays also a role of Ga diffusion barrier [9].

Careful chemical and thermal treatment of the reactor must be carried out after each grow run to prevent residual deposits of HgCdTe on substrate that adversely affect nucleation stage of growth. Different phases on the edges and in the middle of the wafer were frequently observed for poorly cleaned reactor.

Epiready (100) GaAs wafers with 2–4° disorientation towards <100> and <110> have been used. Due to the large mismatch between GaAs and CdTe, both (100) and (111) growth may occur. It mostly depends on substrate disorientation and preparation, nucleation conditions and growth temperature. Cd or Te substrate treatment just before growth results in (100) and (111) orientation, respectively.

Generally, layers with orientation (100) show superior morphology compared to (111) but they are also characterized by hillocks. Height of hillocks is typically twice higher compared to the layer thickness.

Origin of hillocks is not fully understood at present. Hillocks are created during CdTe buffer growth and HgCdTe growth only enlarging them. Epilayers with hillocks are practically useless for device fabrication. Various ways to prevent hillocks formation have been tried: Zinc nucleation layer, different Cd/Te ratios, different substrates orientations have been used, but we were able to grow hillocks-free layers only on some substrates from one supplier (see Fig. 3). Therefore, most of the devices were based on (111) layers.

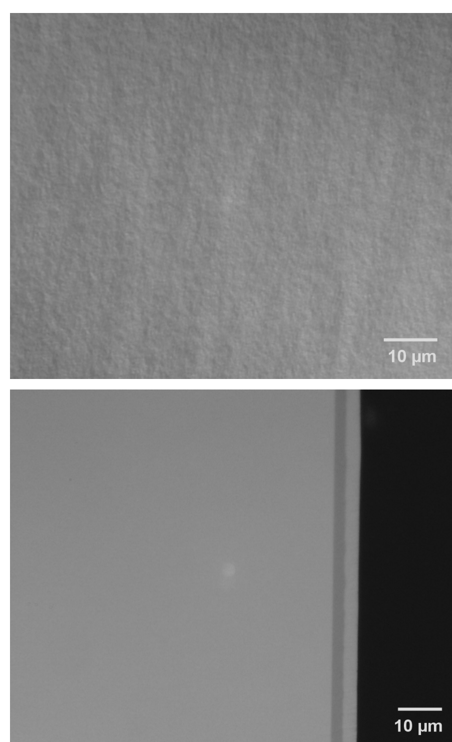

Fig. 3. Surface morphology and cleavage of (100) layer

5. $Hg_{1-x}Cd_xTe$ growth

Direct $Hg_{1-x}Cd_xTe$ growth is difficult due to different thermodynamic properties of HgTe and CdTe [7,10]. We applied interdiffused multilayer process (IMP) for $Hg_{1-x}Cd_xTe$ growth to avoid this problem. IMP gives the possibility for controllable growth of heterostructures with complex composition and doping profiles. HgTe and CdTe layers are deposited one after another with period 100–200 nm and homogenized by interdiffusion during growth. Any composition can be achieved this way by proper selection of HgTe and CdTe layer growth times.

IMP growth depends in a complex way on precursors concentration, flow velocities, growth temperature and many other factors, frequently dependent on the reactor design. A lot of optimization is required to obtain good quality layers.

One of the critical factors is a proper control of precursors delivery to the growth zone. For practical devices we need multilayer heterostructures with uniform lateral composition and doping level within each layer and, at the same time, with sharp interfaces. This implies very thin IMP pairs and quite short times of CdTe and HgTe growth phases. The practical consequence is that IMP times become comparable to the times required for precursor transport from bubblers to the growth zone. The other complications are significant differences in the transport times for different precursors, mixing effects and different carrier gas flow velocities for the CdTe and HgTe growth stages [7]. This may result in poor control of the actual concentration of precursors that could adversely affect the quality, homogeneity and doping of the HgCdTe layers. Reduction of precursor's delivery times is possible with increased carrier gas flow but the shorten residence time of precursors decreases pyrolysis efficiency, which lead to the waste of expensive metalorganic precursors.

The problems described above can be solved to some degree by the use of four-phase IMP process proposed by Svoronos *et al* [11]. The carrier gas flow through DIPTe bubbler is switched on at start of HgTe phase and switched off at the beginning of HgTe flush phase. DIPTe and DMCd bubblers are switched on and off at the start and at the end of CdTe phase, respectively. Typically, the carrier gas flow during CdTe/CdTe flush phase is approximately 4 times longer of that during the HgTe/HgTe flush one [12]. The CdTe phase is usually used also to introduce doping precursors. CdTe growth phase is critical for growth of low composition MCT because of its shortness.

Careful selection of the flows and valve switching times is necessary to ensure optimum growth conditions. Experimental optimization of the growth conditions is costly and time consuming. The theoretical modeling has been used as the first approximation that could be eventually corrected with suitable experiments. Figure 4 shows modeled partial pressures of precursors in growth zone during four-stage IMP. The most simple approximation is the plug flow (PF) model that describes temporal changes of precursor concentration as rectangular pulses characterized by delays compared to the nominal HgTe and CdTe phases (see Fig. 4 – DIPTe PF). This means that the HgTe and CdTe growth occurs partially during the HgTe and CdTe phases, and partially are continued during the flush phases.

The PF model is usually a good approximation of gas flow through a thin pipe but poor for the liner volumes of complex shape, where mixing effects are significant. The mixing effects and changes of carrier gas flow may cause significant distortion of the pulses (Fig. 4). The distortion depends on the design of particular gas system and differs for various precursors.

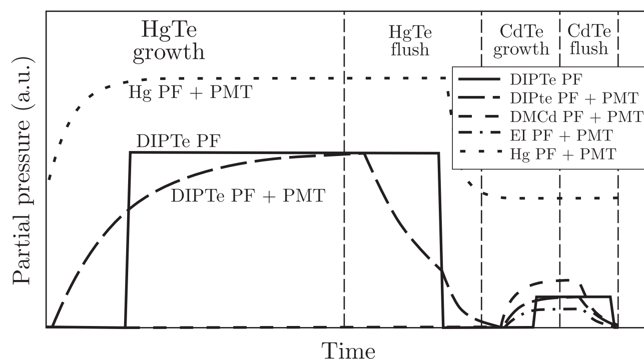

Fig. 4. Modeling precursor concentration during IMP technique. DMCd and DIPTe in scale, Hg scale ×17, EI scale ×200. We assume equal delays for all precursors in CdTe growth phase

1. *HgTe growth phase*
   Low carrier gas total flow velocity causes large delay of DIPTe precursor. Time needed for precursor to pass through pipes from bubbler to reactor is estimated with PF model (DIPTe PF – Fig. 2).
2. *HgTe flush phase*
   Total flow rate is changed during that phase. Increase in total gas flow rate during CdTe phase could cause unstable growth conditions because of changing partial pressure of DMCd and DIPTe at the beginning of CdTe deposition. Time of the flush after HgTe is a compromise. From one hand it must be carefully selected to ensure no residual DIPTe precursor pressure during the CdTe growth phase. From the other hand it must be short enough to avoid evapouration of HgTe. Low residual DIPTe partial pressure after the flush phase is particularly important for doping, where DMCd/DIPTe ratio must be precisely controlled.
3. *CdTe growth*
   CdTe layers deposited during IMP cycle must interdiffuse during next few cycles to ensure composition uniformity. Injected precursors have different delivery times, so they can't be switched on simultaneously. Delays and bad switching moments can cause deterioration of morphology (especially (100) one), inefficient doping, and unintentional DAG.

4. *CdTe flush*
   CdTe flush phase is less critical for growth, because of low evapouration velocity of CdTe.

In practice, the partial pressures of precoursors could be predicted with limited accuracy and the process' design have to be experimentally adjusted. Doping and flushes times are longer than modeling results pointing at. In reality, during IMP the precursors switching are much more complicated. Properties of mass flow controllers forced us to use delta doping to achieve low-doped MCT layers. CdTe growth time is kept constant in all absorber layers. We observed large, nonlinear, composition shifts when we change CdTe growth time, therefore the composition calibration was adjusted through HgTe growth time. We have created library with growth parameters.

Linear deposition characteristics over substrate must be assured to avoid non-uniformity of HgCdTe composition. First of all, deposition characteristics depend on linear flow velocity over substrate.

Figure 5 shows transmission of HgCdTe epilayers. The absorption edge is mostly determined by the layer with the lowest x-value and can be used to determine composition. We can evaluate composition uniformity across the wafer by mapping. The compositional uniformity over the wafer as low as ±0.1% is achieved.

The infrared transmittance spectra of high quality layers are close to the theoretical ones. This is an evidence of good in-depth homogeneity. Complex interferences patterns are observed for long wavelength.

Compositional profiles were evaluated for some samples by differential reflection spectra or with SIMS method.

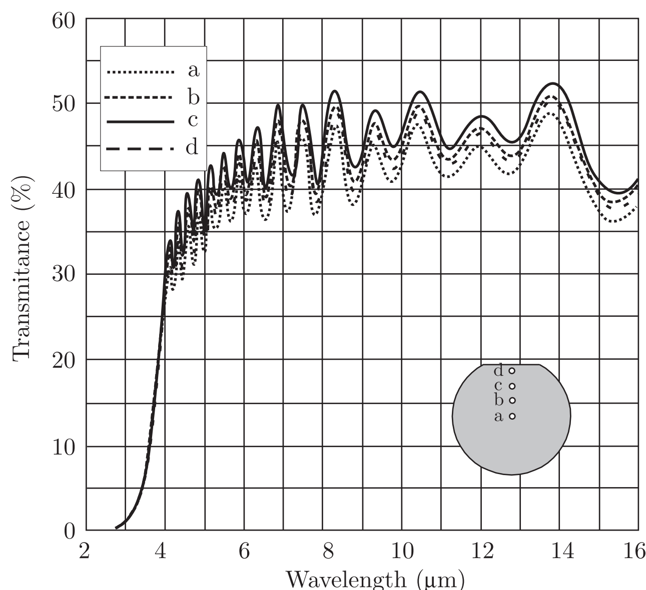

Fig. 5. Infrared transmission spectra of multilayer heterostructure

6. $Hg_{1-x}Cd_xTe$ doping

6.1. Undoped layers. Electrical properties of nominally undoped $Hg_{1-x}Cd_xTe$ layer are determined by native acceptors (metal vacancies) and uncontrolled background doping. Vacancy concentration strongly depends on reactor temperature, vapour pressure and material composition. The native doping level after growth at 360°C with mercury temperature 200°C is approximately 5×10^{16} cm^{-3}. This is much below the expected level of $>1\times10^{17}$ cm^{-3} for this temperature conditions [13]. We suspect that it is due to partial annihilation of vacancies during cool down. It could be influenced by hydrogen presence in the layer.

The vacancy concentration can be changed by post-growth annealing in mercury vapours. Vacancies may be practically eliminated by a prolonged, low temperature (≈200°C) annealing at near saturated mercury pressures. Such annealing reveals the background doping level. We have observed the uncontrolled background about $N_d - N_a = (1-3)\times10^{15}$ cm^{-3} for our MOCVD system.

Ex-situ anneal in sealed quartz ampoules in mercury vapours is typically used to maintain isothermal conditions. This technique is not practical for production purposes. Instead, we developed more convenient *ex-situ* anneal technique in which a wafer after growth was transported into reusable quartz container. Temperatures up to 400°C and Hg pressures up to 2 bars could be used.

High and low temperature annealing was used. Typically, a short (approx. 20 min – 3 h) high temperature (360°C) anneal was used for doping homogenization followed by long (>2 h) low temperature (250°C) anneal for vacancy annihilation. Mercury pressure has been changed during both stages of this annealing to maintain conditions close to isothermal ones.

In-situ annealing is very practical for production purposes. This eliminates the need for any "hot" processes after removal of wafers from the MOCVD reactor, and the possibility to introduce additional impurities. We have developed *in-situ* annealing technique which can be applied for many practical purposes. The annealing is carried out in the reactor immediately after the growth.

When the growth is finished, the temperature of the wafer is gradually lowered to 210°C for 1–6 hours keeping the mercury source temperature at the 200–220°C. After that both reactor and mercury are cooled down. It must be avoided to cool down the rector below the mercury level to prevent Hg droplet formation. During annealing it is not possible to close the reactor and stop hydrogen flow. This result in significant mercury loses. In practice, this means that we cannot obtain near saturated mercury pressures at temperatures >220°C. This effect can be limited by selecting optimal upper to lower channel flow ratio.

Vacancy and background doping is not sufficient for advanced infrared devices that require donor and acceptor doping at medium and high doping levels.

6.2. Doping with foreign impurities. Iodine and arsenic have been used as foreign dopants. Both are well behaved, stable and slowly diffusing dopants. To be active dopants they must occupy Te sites. Metal-rich conditions are favorable for iodine incorporation and are required for arsine. Therefore they have been introduced during CdTe phase with Cd/Te ratio > 1. Most of doping experiments have been carried out for (111) $Hg_{1-x}Cd_xTe$ layers.

Iodine doping. Iodine is well behaved dopant and it is typically used to obtain heavily doped n^+-layers. Therefore it is important to establish conditions for iodine doping at $> 10^{17}$ cm^{-3} level. Cd/Te ratio of 1.1–1.3 has been used during CdTe phase to improve efficiency of I incorporation and activation. It allows doping concentration between 1×10^{17} and 1×10^{18} cm^{-3} for the compositions of about 0.3.

Multi-level staircase structure quickly yielded dopant source calibration curves. Figure 6 shows calibration structure obtained using ethyliodode (EI) which was assessed by SIMS measurements and differential 77K Hall profiling. The obtained correlation between the electrical and chemical results implied the iodine incorporated on the correct Te lattice site; and that within the accuracy of the techniques, the activation efficiency is close to 100%. However, along with increasing iodine concentration its activation decreases. Probably for high iodine concentration it starts to occupy interstitials or metal sites. Although EI shows the desirable properties of a donor dopant source, the minimum EI concentration about 0.2 ppm could be obtained with sensible choices of source temperature and double dilution mass flow controllers (MFC) settings. The range of 0.05 ppm (first step at calibration structure) was obtained by setting very short injection times to the reactor – 0.4 s of EI. The control of iodine concentration is difficult below 1×10^{16} cm^{-3}.

Improved efficiency of doping has been observed with *ex-situ* annealing at 360oC at near saturated mercury pressures. This effect may be related to incomplete iodine homogenization during growth and *in-situ* annealing, since iodine diffusion is very slow (noticeably slower then Cd diffusion into HgTe).

Heterostructure photovolataic IR detectors require heavily doped n^+-layers with relatively high x composition ($x > 0.45$). It is expected that such layers should have resistivity as small as possible to provide good electrical contact. Until now, the $Hg_{1-x}Cd_xTe$ layers with composition $x > 0.45$ doped with EI doses above 10 ppm had electron concentration lower than 7×10^{17} cm^{-3} and sheet resistance above 10 Ω. These parameters indicate that significant part of iodine atoms are not located in Te lattice and are not electically active. Preliminary experiments with increasing Cd/Te ratio and *ex-situ* annealing have not improved EI doping noticeably. No or insignificant I doping memory effects have been observed. Good reproducibility of I doping has been observed.

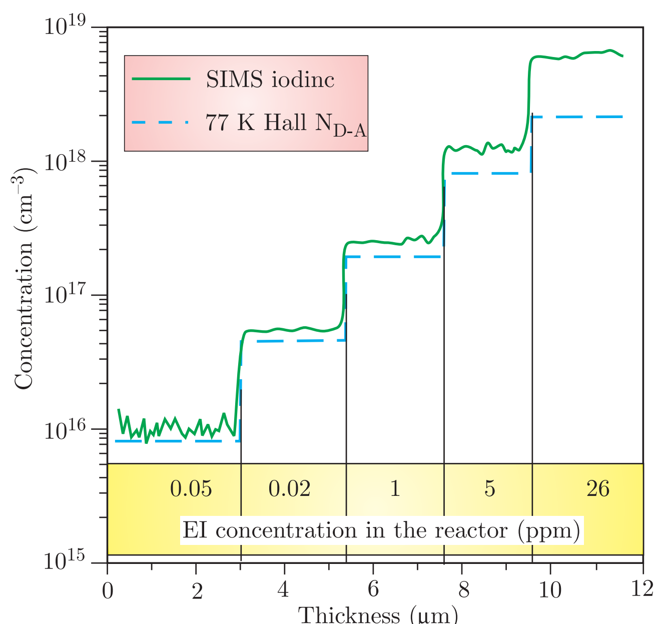

Fig. 6. Calibration profile of staircase structure doped using ethyliodide. Composition $x = 0.30$

Arsenic doping. Arsine incorporation into Te sites is very sensitive for metallic rich conditions. This assures conditions for arsenic to enter Te sites where it acts like an acceptor. Otherwise arsenic can show amphoteric behavior.

High doping concentrations ($> 5\times10^{17}$ cm^{-3}) have been achieved in higher x materials ($x > 0.25$) with Hg temperature 220°C and arsine fraction of 10 ppm. It is much more difficult to achieve heavily doped low x materials. Arsenic incorporates only during CdTe cycle in IMP growth process. The growth time of CdTe cycle (the active time of As doping) is considerably shorter than HgTe cycle for low x layers. As a result, the relative arsenic incorporation is worse in epilayers with low x compositions than in high x ones. The investigation of optimal growth conditions for more effective doping in low x layers is still continued. So far concentrations of up to 2×10^{17} cm^{-3} have been achieved for mercury temperature of 220°C, Cd/Te ratio equal to 5 and arsine fraction of 5 ppm in the growth zone.

High doping concentrations ($> 5\times10^{17}$ cm^{-3}) have been achieved in higher x materials ($x > 0.25$) with Hg temperature 220°C and arsine fraction of 10 ppm. It is much more difficult to achieve heavily doped low x materials. concentrations up to 2×10^{17} cm^{-3} have been achieved for mercury temperature of 220°C, Cd/Te ratio equal 5 and arsine fraction of 4 ppm in the growth zone.

Figure 7 shows the efficiency of arsenic doping as a function of AsH_3 partial pressure for two crystallografic orientations: for the (100) and (111). Different orientations were obtained by different nucleation conditions. The difference in doping efficiency for the two orientations is clearly evident, with near an order of magnitude higher incorporation rate in (100) orientation. The detailed explanation of this phenomenon is presented in [14].

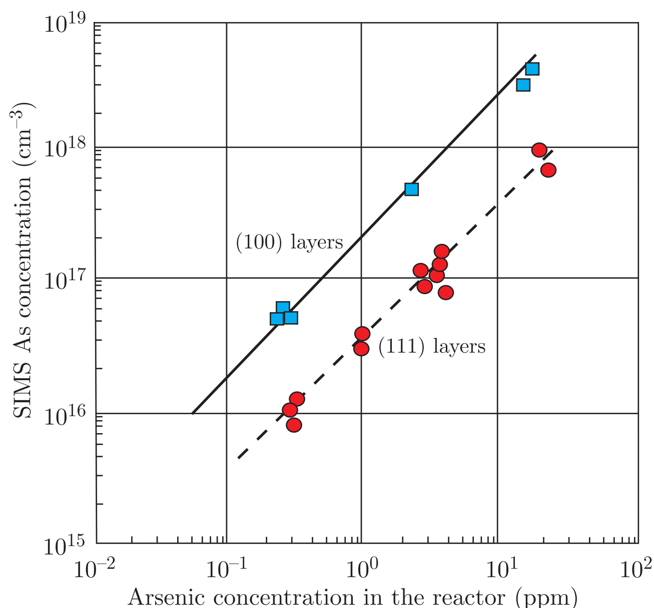

Fig. 7. Arsenic incorporation in HgCdTe vs AsH_3 partial pressure, measured by SIMS, for the (100) and (111) orientations. Composition $x = 0.28$–0.33

Ex-situ isothermal annealing in high mercury vapours (360/350°C) shows significant effects on acceptor doping. It is probably related to arsenic activation in the material.

Strong dependence of CdTe growth rate was visible for different arsine concentrations. It is between 4 and 8 μm/h and it strongly depends on dopants partial pressures.

7. Uncooled HgCdTe devices with improved performance

The class of photon detectors is sub-divided into different types depending on how the electric or magnetic fields are developed. Initial efforts to produce near room temperature LWIR photon detectors have concentrated mainly on optimization of photoconductors and PEM detectors. More information can be found in previously published papers [1,3,15]. The room temperature photovoltaic device of conventional design suffers from

— poor quantum efficiency, and
— low differential resistance.

Only charge carriers that are photogenerated at a distance shorter than the diffusion length from junction can be collected. The absorption depth of long wavelength IR radiation ($\lambda > 5$μm) is longer than the diffusion length. Therefore only a limited fraction of the photogenerated charge contributes to the quantum efficiency. Let us onsider an example of an uncooled 10.6 μm photodiode. The calculations show that the ambipolar diffusion length is less than 2 μm while the absorption depth is ≈ 13 μm. This reduces the quantum efficiency to ≈ 15% for single pass of radiation through the detector.

The resistance of the p-n junction is very low due to a high thermal generation. In the materials with a high electron to hole mobility ration, the resistance is additionally reduced by ambipolar effects [16] As a result, the preamplifier noise and noise of parasitic resistances may exceed the thermal generation-recombination noise. Thus, the performance of conventional devices is very poor, so they are not usable for practical applications.

The present generation of uncooled LWIR devices is based on photovoltaic devices [17–22] The problems of poor quantum efficiency and large series resistance have been solved through adoption of sophisticated heterojunction architectures of photovoltaic devices in combination with the methods of reduction of physical size of an active element.

An efficient improvement was development of multiple heterojunction photovoltaic devices to increase the voltage responsivity of the devices. Practical realization of the multi-heterojunction device that is consisted of a structure based on backside illuminated n^+-p-P photodiodes (symbol "+" denotes strong doping, capital letter – wider gap) have been presented in several papers [17–21] The individual detector elements were prepared by a combination of conventional dry etching, angled ion milling, and angled thermal evapouration for contact metal deposition (see Fig. 8). p-type active layer with thickness of approximately 3 μm and doping levels of about 10^{16} cm^{-3} were grown on GaAs substrates using MOCVD and *in-situ* As doping. The delineation trenches in the epilayer were wet chemical etched using Br/ethylene glycol or Br/HBr solutions to a depth of 2/3 of the thickness of epilayer. The etch was followed by shallow ion beam milling using a Kaufman-type ion gun. The sample was placed at ≈ 45° to the direction of the Ar^+ beam so that only one wall of the trench was exposed to the beam. The ion beam milling results in n-type conversion and the formation of n^+-p junctions on the uppermost surface and on one side of the trench walls. Due to the grading of the epilayer composition and doping with depth, the final structure approximates an n^+-p-P^+ photodiode. Cr/Au metallization was required to provide external contact to the device and to short-circuited n^+-p junction formed at the base of trench, effectively connecting side-by-side diodes in series. As a final step, the devices were passivated by thermal evapouration of 200 nm of CdZnTe followed by 300 nm of ZnS. For an ≈3-μm thick epilayer, the minimum practical multijunction period using existing wet etching technology is ≈10 μm.

The critical issue of multiple HgCdTe photodiodes may arise from requirement of a very small size of individual element (for LW room temperature devices the optimum length of an individual element is below 5 μm) which makes difficult to achieve a high ratio of the active to the dead areas. Moreover, such devices suffer from the non-uniform response across the active area. These problems have been mostly overcome and the devices are commercially available at present. The devices are manufactured as single devices optimized for any wavelength

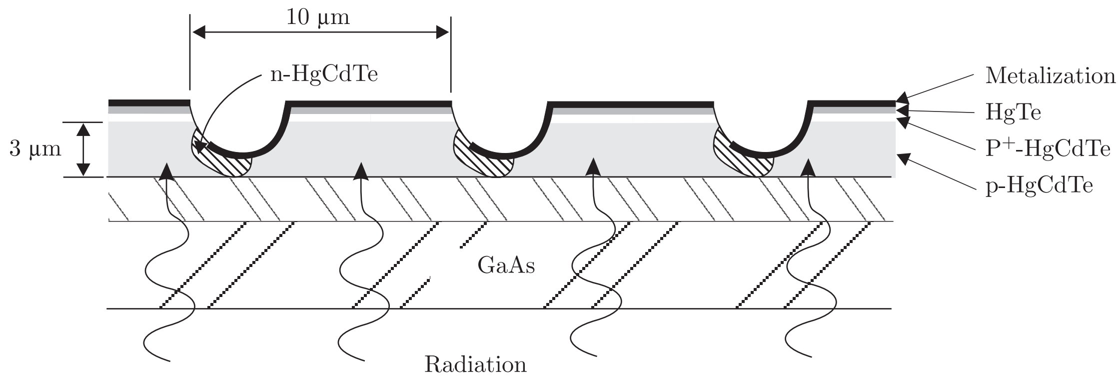

Fig. 8. Backside illuminated multiple heterojunction device

within the 2–16 μm range, with active area sizes from a few micrometers to a few millimeters. Linear arrays up to 120 elements and small 2D arrays are manufactured as custom devices.

Figure 9 shows the room temperature spectral response of HgCdTe multi-heterojunction devices monolithically immersed to the CdZnTe lens. The devices were based on multiple junctions with a period of 10 μm. Generally, these room temperature devices have responsivities that are comparable to, or better than, photoelectromagnetic devices operating under the same conditions. Peltier cooled devices exhibit performance that is comparable to photoconductors operating at the same wavelength and temperatures. However, in contrast to photoconductors, multi-heterojunction detectors can be used at both low and very high frequencies. Heterodyne experiments indicate that the response time of LWIR devices at a wavelength of 10.6 μm is only of about 1 ns.

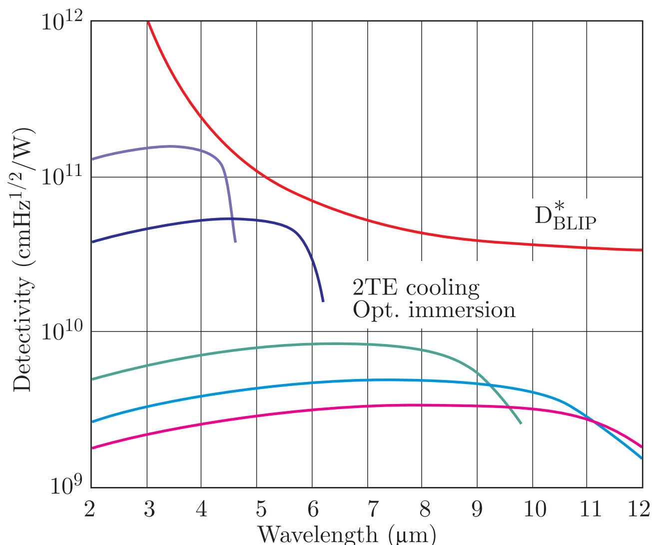

Fig. 9. Measured detectivity of multi-heterojunction uncooled HgCdTe detectors; optical immersion has been used to improve the performance

Without optical immersion, photovoltaic detectors are sub-BLIP devices with performance close to the generation-recombination limit. Well designed optically immersed devices when thermoelectrically cooled with 2-stage Peltier coolers, show detectivities up to 10^{11} $cmHz^{1/2}/W$ at 5 μm, closely approaching the BLIP limit.

Situation is less favorable for LWIR photovoltaic detectors. Detectivities exceeding 1×10^9 $cmHz^{1/2}/W$ and $\approx 6\times10^9$ $cmHz^{1/2}/W$ have been measured with uncooled $\lambda = 8.5$ μm non-immersed and optically immersed devices, respectively. Optically immersed 10.6 μm PV devices cooled with 2-stage Peltier cooler with detectivities $> 4\times10^9$ $cmHz^{1/2}/W$ has been also measured. Despite of all improvements (advanced architecture, optical immersion, Peltier cooling) they show detectivities below the BLIP limit by almost one order of magnitude.

The devices are especially promising as uncooled 7.8–9.5-μm detectors that can be used for thermal imagers. Initial results are encouraging, indicating the potential for achieving $\approx 10^9$ $cmHz^{1/2}/W$ at $\lambda \approx 9$ μm. This would enable thermal resolution better than 0.1 K for staring thermal imagers operating with f/1 optics. Moreover, the devices exhibit very fast response with a time constant of ≈ 1 ns. This is due to the short time required for photogenerated carriers in small size active region to reach heavily doped contacts and a short RC time constant as well.

The frequency response of photovoltaic devices is limited by transport of photogenerated charge carriers through the absorber region and by RC time constant. Transport through the absorber region is a combination of diffusion and drift. The p-type $Hg_{1-x}Cd_xTe$ is the material of choice for an absorber of a fast photodiode due to a large diffusion coefficient of electrons. The diffusion transit times are ≈ 100 ps for extrinsic p-type 2-μm thick $Hg_{0.82}Cd_{0.18}Te$ absorber. Further reduction can be achieved with thinner absorber. Drift transport in reverse biased devices can further reduce the transit time.

The main limitation of response time is usually the RC time constant. For transimpedance preamplifier with a low input resistance, the RC time constant is determined by the junction capacitance and the photodiode series resistance. Reduction of series resistance by almost two

orders of magnitude is possible using the structures with heavily doped n-type material for the mesa base layer, with corresponding reduction of the *RC* time constant.

Very short *RC* time constant is expected in optically immersed photodiodes with a very small area of an active region. With these improvements, photodiodes can be use for gigahertz range detection of IR radiation.

Optical immersion has been used almost exclusively for single element devices. The use of a single immersion lens to a large array is problematic in view of optical aberrations and the large lens size. The problem can be solved by implementation of a small size 2D array monolithically integrated with microlenses matrix. The small size of active element ($\approx 7\times7$ μm) is beneficial for good collection of photogenerated charge carriers especially in LWIR devices. The individual elements can be accessed individually or connected in series.

8. Conclusions

Practical implementation of the advanced photodetector architecture requires well established epitaxial technology. In Poland, for a long time, the isothermal vapour phase epitaxy (ISOVPE) in reusable growth system was used in VIGO System S.A. to grow HgCdTe heterostructure devices. Now, the ISOVPE has been replaced with MOCVD (a common investment of VIGO System and Military University of Technology, Warsaw). This technique has been selected for its inherent versatility (low growth temperature, ability to grow layered structures with complex composition and doping profiles while maintaining sharp interfaces). MOCVD makes possible to use low-cost and high quality substrates (GaAs, sapphire and silicon), has the potential for a large-scale production and is cost-effective. Physical properties of MOCVD HgCdTe heterostructures on GaAs substrates exceed those on costly CdTe substrates.

HgCdTe heterostructures have been grown on 2" (100)GaAs. Reproducible n- and p-type doping at the low, intermediate and high level (10^{15}–10^{18} cm^{-3}) has been achieved with stable iodine and arsenic dopants. The dopants are easily activated during growth in contrast to MBE. This technology is used for photoconductive, photoelectromagnetic, and photovoltaic HgCdTe devices.

The present generation of uncooled LWIR devices is based on photovoltaic devices. The problems of poor quantum efficiency and large series resistance have been solved through adoption of sophisticated multiheterojunction architectures in combination with the methods of reduction of physical size of an active element. These devices are especially promising as uncooled 7.8–9.5-μm detectors that can be used for thermal imagers. Initial results are encouraging, indicating the potential for achieving $\approx 10^9$ cmHz$^{1/2}$/W at $\lambda \approx 9$ μm. Near-BLIP performance is possible at ≈ 230 K with optical immersion.

Acknowledgements. This work was supported by the Polish Ministry of Science and Information Technology in the frame of the Project No. PBZ-MIN-009/T11/2003.

References

[1] J. Piotrowski, W. Galus and M. Grudzień, "Near room-temperature IR photodetectors", *Infrared Phys.* 31, 1–48 (1990).

[2] J. Piotrowski, "Uncooled operation of IR photodetectors", *Opto-Electron. Rev.* 12, 111–122 (2004).

[3] J. Piotrowski and A. Rogalski, "Uncooled long wavelength infrared photon detectors", *Infrared Phys. Technol.* 46, 115–131 (2004).

[4] K. Adamiec, M. Grudzień, Z. Nowak, J. Pawluczyk, J. Piotrowski, J. Antoszewski, J. Dell, C. Musca and L. Faraone, "Isothermal vapour phase epitaxy as a versatile technology for infrared photodetectors", *Proc. SPIE* 2999, 34–43 (1997).

[5] P. Norton, "HgCdTe infrared detectors", *Opto-Electron. Rev.* 10, 159–174 (2002).

[6] L. Colombo, R.R. Chang, C.J. Chang, and B.A. Baird", Growth of Hg-based alloys by the travelling heater method," *J. Vac. Sci. Technol.* A6, 2795–2799 (1988).

[7] S.J.C. Irvine, "Metal-organic vapour phase epitaxy", *Narrow-gap II–VI Compounds for Optoelectronic and Electromagnetic Applications*, pp. 71–96, edited by P. Capper, Chapman & Hall, London, 1997.

[8] O.K. Wu, T.J. de Lyon, R.D. Rajavel, and J.E. Jensen, "Molecular beam epitaxy of HgCdTe", in *Narrow-Gap II–VI Compounds for Optoelectronic and Electromagnetic Applications*, pp. 97–130, edited by P. Capper, Chapman & Hall, London, 1997.

[9] W.E. Tennant, C.A. Cockrum, J.B. Gilpin, M.A. Kinch, M. B. Reine and R. P. Ruth "Key issues in HgCdTe-based focal plane arrays: An industry perspective", *J. Vac. Sci. Technol.* 10, 1359–1369(1992).

[10] L.M. Smith and J. Thompson, "Metal organic chemical vapour deposition (MOCVD) of cadmium telluride, mercury telluride and cadmium mercury telluride", *Chemtronics* 4, 60 (1989).

[11] S.A. Svoronos, W.W Woo, S.J.C. Irvine, H.O. Sankur, and J. Bajaj, "A model of the interdiffused multilayer process", *J. Electron. Mater.* 25, 1561–1571 (1996).

[12] C. Theodoropoulos, N.K. Ingle, and T.J. Mountziaris: "Computational studies of the transient behavior of horizontal MOVPE reactors", *J. Cryst. Growth* 170, 72–76 (1997).

[13] H.R. Vydyanath, "Donor and acceptor dopants in $Hg_{1-x}Cd_xTe$ alloys", *J. Vac. Sci. Technol.* B9, 1716–1723 (1991).

[14] L. Svob, I. Cheye, A. Lusson, D. Ballutaud, J.F. Rommeluere and Y. Marfaing, "Crystallographic orientation dependence of As incorporation in MOVPE-grown CdTe and corresponding acceptor electrical state activation", *J. Cryst. Growth* 184/185, 459–464 (1998).

[15] J. Piotrowski and A. Rogalski, "Photoelectromagnetic, magnetoconcentration and Dember infrared detectors" in *Narrow-Gap II–VI Compounds and Electromagnetic Applications*, pp. 506–525, edited by P. Capper, Chapman & Hall, London 1997.

[16] J. Piotrowski, W. Gawron, and Z. Djuric, "New gen-

eration of near-room-temperature photodetectors", *Opt. Eng.* 33, 1413–1421 (1994).

[17] J. Piotrowski and W. Gawron, "Extension of longwavelength IR photovoltaic detector operation to near room-temperatures", *Infrared Phys. Technol.* 36, 1045–1051 (1995).

[18] C. Musca, J. Antoszewski, J. Dell, L. Faraone, J. Piotrowski, and Z. Nowak, "Multi-heterojunction large area HgCdTe long wavelength infrared photovoltaic detector for operation at near room temperature", *J. Electron. Mater.* 27, 740–746 (1998).

[19] J. Piotrowski, Z. Nowak, J. Antoszewski, C. Musca, J. Dell, and L. Faraone, "A novel multi-heterojunction HgCdTe long-wavelength infrared photovoltaic detector for operation under reduced cooling conditions", *Semicond. Sci. Technol.* 13, 1209–1214 (1998).

[20] W. Gawron and A. Rogalski, "HgCdTe buried multijunction photodiodes fabricated by the liquid phase epitaxy", *Infrared Phys. Technol.* 43, 157–163 (2002).

[21] J. Piotrowski, M. Grudzień, Z. Nowak, Z. Orman, J. Pawluczyk, M. Romanis, and W. Gawron, "Uncooled photovoltaic $Hg_{1-x}Cd_xTe$ LWIR detectors", *Proc. SPIE* 4130, 175–184 (2000).

[22] J. Piotrowski, P. Brzozowski, and K. Jóźwikowski, "Stacked multijunction photodetectors of long wavelength radiation", *J. Electron. Mater.* 32, 672–676 (2003).